

DESIGN AND CONSTRUCTION OF A BENDING-ACTIVE METAMATERIAL PLYWOOD STRUCTURE: THE FLEXMAPS PAVILION

Francesco LACCONE¹, Luigi MALOMO², Marco CALLIERI³, Thomas ALDERIGHI⁴, Alessandro MUNTONI⁵, Federico PONCHIO⁶, Nico PIETRONI⁷, Paolo CIGNONI⁸

¹Postdoctoral Researcher, ISTI - CNR, Via Moruzzi 1, 56124 Pisa, Italy, francesco.laccone@isti.cnr.it

²Researcher, ISTI - CNR, Via Moruzzi 1, 56124 Pisa, Italy, luigi.malomo@isti.cnr.it

³Senior Researcher, ISTI - CNR, Via Moruzzi 1, 56124 Pisa, Italy, marco.callieri@isti.cnr.it

⁴PhD student, ISTI - CNR, Via Moruzzi 1, 56124 Pisa, Italy, thomas.alderighi@isti.cnr.it

⁵Technologist, ISTI - CNR, Via Moruzzi 1, 56124 Pisa, Italy, alessandro.muntoni@isti.cnr.it

⁶Researcher, ISTI - CNR, Via Moruzzi 1, 56124 Pisa, Italy, federico.ponchio@isti.cnr.it

⁷Senior Lecturer, University of Technology Sydney, 81 Broadway, Ultimo NSW, Australia, nico.pietroni@uts.edu.au

⁸Research Director, ISTI - CNR, Via Moruzzi 1, 56124 Pisa, Italy, paolo.cignoni@isti.cnr.it

Editor's Note: This space reserved for the Editor to give such information as date of receipt of manuscript, date of receipt of revisions (if any), and date of acceptance of paper. In addition, a statement about possible written discussion is appended.

DOI: Digital Object Identifier to be provided by Editor when assigned upon publication

ABSTRACT

Metamaterial is a modern and efficient design concept based on designing the geometry of structural material at the meso-scale to achieve desired mechanical performances. In the context of bending-active structures, such a concept can be used to control the flexibility of the panels forming a surface without changing the constituting material. These panels undergo a formation process of deformation by bending, and application of internal restraints. This paper describes a new constructional system, FlexMaps, that has initiated the adoption of bending-active metamaterial structures at the architectural scale. Here, metamaterial modules are in the form of four-arms spirals made of CNC milled plywood and are designed to reach the desired target shape once assembled. All phases from the conceptual design to the fabrication are seamlessly linked within an automated workflow. To illustrate the potential of the system, the paper discusses the results of a demonstrator project entitled FlexMaps Pavilion (3.90x3.96x3.25 meters) that has been exhibited at the IAASS Symposium in 2019 and more recently at the 2021 17th International Architecture Exhibition, La Biennale di Venezia. The structural response is investigated through a detailed structural analysis, and the long-term behavior is assessed through a photogrammetric survey.

Keywords: *Bending-Active Structures, Computer Aided Design, Optimization, Shell Structures, Timber Spatial Structures, Structural Design*

1. INTRODUCTION

In all manufacturing fields, a large transition is taking place from the philosophy of mass production and modularity to the extreme customization of products. This transition is supported by an expanded availability of new computational tools and by the possibilities introduced by numerically-controlled machines, like cutters and material extruders. Research and practice in the architectural and structural fields are also moving in this direction. In such cases, the customization can be oriented towards aesthetics, shape requirements, mechanical performance (i.e. high strength or stiffness), and

accomplishment of sustainability goals (i.e. material reduction or reuse) [1-9].

Based on these premises, workflows that seamlessly link design with physical production have become necessary to combine the multiple goals and constraints in a closed optimization loop. In particular, new techniques have been introduced for reinterpreting or abstracting the objects in a new style [10], preserving their shape or desired functions.

Metamaterials are man-made structures that can be regarded as an abstraction of continuous bodies.



Figure 1: The FlexMaps Pavilion at the at the Competition and exhibition of innovative lightweight structures, Form and Force, joint international conference of IASS Symposium 2019 and Structural Membranes 2019, and at the 2021 17th International Architecture Exhibition, La Biennale di Venezia.

They are designed at the meso-scale in order to achieve a desired mechanical performance [11]. The macroscopic behavior of these structures is mainly determined by the arrangement of the solid material rather than only their chemical matrix at the micro-scale. Surface metamaterials that can be bent and stretched to deform into a pre-described shape can be used to form the skin of an object. In this case, the stiffness of each part is to be designed with respect to the target shape objective and to form a consistent structural assembly as a whole, i.e. stable, resistant and stiff.

This mechanical formation process of deforming a body and constraining it to form a certain shape is shared with the bending-active structures. Actively bending is an approach to build curved architectural surfaces made of flat, linear or planar, elements, which are designed to support an internal pre-stress derived from an imposed curvature during the assembly process [12-18]. Boundary constraints and internal joints lock the position of the elements once the desired spatial configuration is reached.

The form-finding of bending-active structures requires geometry- and physically-based methods to predict the deformation and the material stress at each stage of the formation process [19]. However, due to the complexity of this problem, only a few methods are sufficiently generic to allow imposing a target shape and finding the best arrangement of bending-active components to approximate it [20-22].

This paper reports on the knowledge acquired from the design, analysis, and construction of a bending-

active metamaterial structure entitled FlexMaps Pavilion, which is based on the computational framework of [23]. This prototype is shaped as a thin twisted strip composed of actively-bent patches, which embed carved spiral patterns made of plywood that serve as metamaterial.

This prototype has been created specifically for the “Competition and exhibition of innovative lightweight structures” organized in 2019 by the IASS Working Group 21 “Advanced manufacturing and materials” [24]. After this successful installation at the IASS, which was awarded the First Prize, it was selected to be exhibited within the Italian Pavilion of the 2021 17th International Architecture Exhibition, La Biennale di Venezia from May 22 to November 21, 2021 (Fig. 1). This venue has required a deeper understanding of the structure’s long-term behavior and the elaboration of a monitoring plan to assess the safety level during the exhibition.

The structure design and construction are based on the following automated steps:

- (i) the computational design, which outputs the decomposition of the shape into flat fabricable patches and computes the spiral metamaterial patterns;
- (ii) the detailed structural analysis;
- (iii) the fabrication through CNC milling machines and the instructions for the assembly and monitoring;
- (iv) the monitoring of the shape by means of photogrammetry survey.

Starting from the lesson learned from the IAASS 2019 experience, the analysis of the FlexMaps Pavilion has been revisited considering the requests of the 2021 Venice Biennale exhibition, in which the structure performs as a freestanding indoor installation and is located on a stiff basement provided by the host. The whole assembly composed by the structure and the basement is simply laid on the floor.

2. MATERIALS AND METHODS

A unique workflow links all the main design and construction steps to deliver the FlexMaps Pavilion, as shown in Fig. 2.

The target shape constitutes the main input and can be obtained with any form-finding technique or be generic, i.e. conceived with a sculptural approach. As a lattice structure, the primary requirement for the shape is to be stable. From a theoretical point of view, there are no other restrictions for the shape, i.e. on the topology, Gaussian curvature, supports location. Practically, since the spirals form a discrete system, their size influences the method's capacity to approximate folds and sharp features, which cannot be included without expecting a large shape deviation. Additionally, the material can only attain a limited strength, so the spirals cannot be bent beyond the material capacity without breaking them. So, curvature beyond the material capacity is not allowed. The target shape of the FlexMaps Pavilion is a non-developable twisted strip with a variable curvature from point to point, which has been sculpturally designed to challenge the IAASS 2019 competition requirements of fitting a maximum volume of 4.00 x 4.00 x 4.00 meters.

Other preliminary information and actions are required to initiate the computational design, such as the mechanical characterization of the material to be used and the fabrication setup knowledge (machine operations and tolerances).

The core process of the workflow lies in the computational design, in which the optimal metamaterial decomposition is found. Essentially, an inverse design problem is solved: given a continuous target shape and a set of geometrical and mechanical parameters, find of a set of spiral patches that once bent and assembled result as close as possible to the target shape if submitted to a given load. The general framework behind this process has been extensively described and investigated in [23], and it is recalled in Sec. 3 discussing the input values used for the

specific application of the FlexMaps Pavilion.

A detailed structural analysis is performed to assess the safety level under the requirements of the Biennale exhibition. The model is automatically built from the output of the previous step and is made of 3D brick finite elements with orthotropic material properties. The results are included and discussed in Sec. 4.

The construction of the demonstrator builds directly on the output of the computational design step as well. All the elements to be fabricated are elaborated as a CAM for CNC milling machines. Handling the flat fabricated elements is sufficiently easy, while the most difficult step of the work is the assembly (and disassembly), that being a manual process requires experience. Several undesired failures may happen.

The assembly is designed to be carried out without shape control, so that the accuracy of the final shape solely relies on the self-formation capacity of the structure. The photogrammetry survey is used to prove this accuracy, and it is later adopted to monitor the long-term displacements of the structure submitted to the exhibition conditions, i.e. constant load in humid environment.

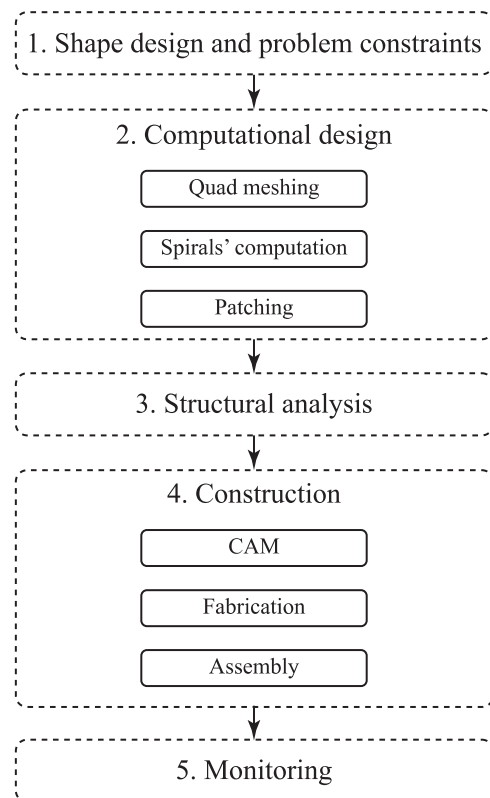


Figure 2: Design workflow of FlexMaps structures.

2.1. System features

FlexMaps structures are thin metamaterial surfaces that can have free-form geometry. These surfaces are made of metamaterial elements shaped as four-arms spirals arranged on a grid, i.e. embedded in a quad mesh. Although they form a 3D configuration, the spirals are fabricated from flat material sheets and then actively bent and mutually connected (Fig. 3).

The spirals define not only the unique aesthetics of the shell but also the proper load-bearing system. Each spiral is computationally designed through a bespoke algorithm that modifies its geometrical features without changing the constituent material, such that, once bent and connected to the neighboring ones, it assumes a predetermined configuration under permanent load.

In the case of the FlexMaps Pavilion the spirals have approximately an equal size of about 0.25 x 0.25 m, but different twist. This is equivalent to having different tiles with a custom stiffness, which have a differentiated attitude in bending. The bending is a self-formation process and introduces a state of pre-stress on the material.

For both shape accuracy and fabrication feasibility, the whole surface is required to be segmented. Thus, each patch is a fabricable module that is obtained out of flat material.

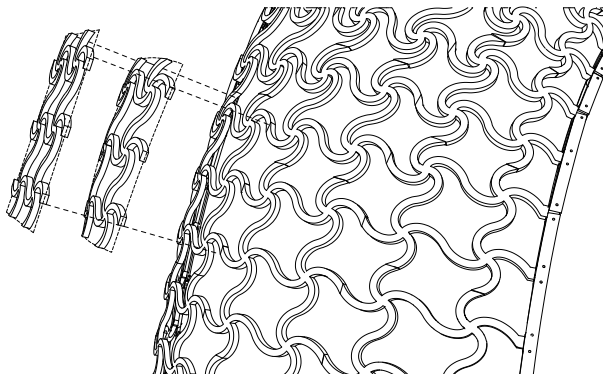


Figure 3: FlexMaps system description: the patches are fabricated as flat elements, then bent and assembled.

2.2. Detailed design

The structure is entirely made of Okumé plywood, which is CNC milled in shop from sheets of 20 mm thickness. The structure is a single-layer piecewise twisted shell that fits a bounding box of 3.90 x 3.96 x 3.25 meters. This shape is non-trivial and non-developable, so it requires to be segmented in several patches in order to be fabricated as flat elements. The Gaussian curvature of the shape is highly variable

from positive values, close to the supports, to negative values in the central part, where the twist takes place.

Spiral-to-spiral joints are located along the seams of the patches and are made of key connector, shown in Fig. 4 (a). These connectors are placed on the spiral arms endpoints and are carved to have an interlocking shape that restrains any relative movement between the parts once assembled. Additionally, this interlocking shape is secured by two M5 bolts coupled with large washers, installed on precision-drilled holes located at the interface of the shape. The bolts thus enhance the shear and bending strength of the connection and guarantee its full-strength.

To restrain the structure's free boundaries, edge beams are provided, as in Fig. 4 (b). These devices consist of a couple of 8 mm lamellae that clamp the boundary connector by means of two bolts. These lamellae are designed as developable strips that are fabricated as flat pieces and then actively bent during the assembly.

To secure the structure to the supports, the spiral arms pointing down are in-plane shaped as T profiles. These are included within a ground beam, as shown in Fig. 4 (c), which is made of three plies of 20 mm plywood. The two lower ones restrain the in-plane position of the T connector, the upper ply locks the T and avoids the uplift.

Originally in the IASS exhibition, the two ground beams were mutually connected only through a plywood paving with the role of balancing the thrust and twisting forces. This paving is made of variable-density Voronoi tiles with a decreasing size from the supports to the center. The edges of the Voronoi polygons are dry interlocking (Fig. 5) and the paving is linked to the ground beams by means of dovetail joints. At the Biennale, due to the increased exhibition time span, the ground beams are rigidly fixed on a supporting platform. However, the paving has been kept as an additional safety measure and for aesthetic reasons. The assembly composed by the structure and the supporting platform constitutes a self-equilibrated system, which is simply laid on the existing concrete paving. The structural cross sections adopted in this work are:

- 20 x 20 mm for the spiral panels;
- two lamellae of 20 x 8 mm for the edge beams;

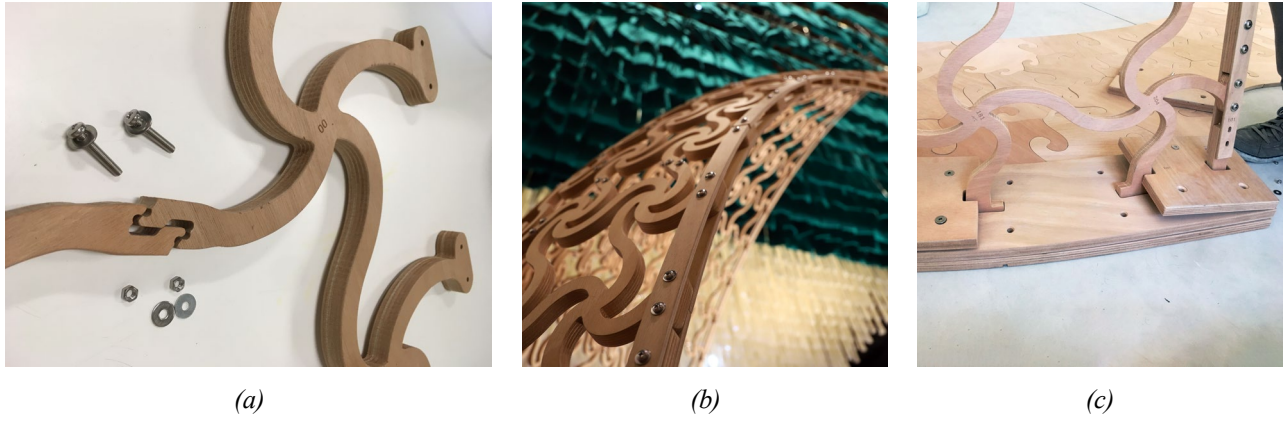


Figure 4: Detailed design of FlexMaps system: (a) patch-to-patch joint; (b) free boundaries joint; (c) supports joint.

- three plies of 200 x 20 mm for the ground beams;
- 12-mm-thick paving tiles.

2.3. Materials

The plywood material adopted in this work is for both general purpose use (non-structural application) and structural application in dry, humid, or exterior conditions (EN 636:2012). To comply with the environmental conditions of the exhibition, a Service Class 2 is adopted as per EN 1995-1-1 (use in humid conditions). The material is Okumé plywood, whose performances as declared by the manufacturer are included in Tab. 1.

Table 1: Material parameters deduced from the manufacturer technical data.

Thickness (mm)	Service Class	Strength	Young's modulus
20 mm	Class 3	42 N/mm ²	4200 N/mm ²

The material is classified Bending strength class F25 and Modulus of elasticity in bending class E40 (EN 636:2012+A1:2015) in both the directions of the grain and perpendicular to the grain of the outer layer of plywood. The characteristic values of the mechanical properties are derived by cross-referencing with EN 12369-2.

The density of $\rho_{w,mean} = 500 \text{ kg/m}^3$ is determined according to EN 323. The strength properties are computed as $X_d = k_{mod} X_k / \gamma_M$, in which X is the generic parameter, $k_{mod} = 0.6$ for permanent loads, and $\gamma_M = 1.2$. The mean stiffness values consider the effect of load duration and humidity. Consequently, the adopted design values in both the direction of the fibers and perpendicular to the fibers are:

$$E_d = 1333.4 \text{ N/mm}^2$$

$$G_d = 150 \text{ N/mm}^2$$

$$f_{b,d} = 16.7 \text{ N/mm}^2$$

$$f_{t-c,d} = 8.3 \text{ N/mm}^2$$

$$f_{v,d} = 2.86 \text{ N/mm}^2$$



Figure 5: Variable-density interlocking Voronoi paving tiles.

2.4. Loads acting on the structure

In the present work, applicable actions are taken into account according to EN 1991-1-1, EN 1991-1-3 and EN 1991-1-4. Moreover, these loading are complying with EN 13782:2015, being the present structure a temporary installation. The main actions are permanent loads and pre-stress. The first ones are computed as characteristic value from the dead load due to self-weight. The second ones are deduced from the simulation of the bending of patches, which collects the story of deformation and stress from flat to their final configuration.

Variable actions are introduced as horizontal loads. The installation is not accessible to visitors, which can only walk around the structure without touching it nor walking through it nor on the supporting platform. For the sake of safety, a minimum amount

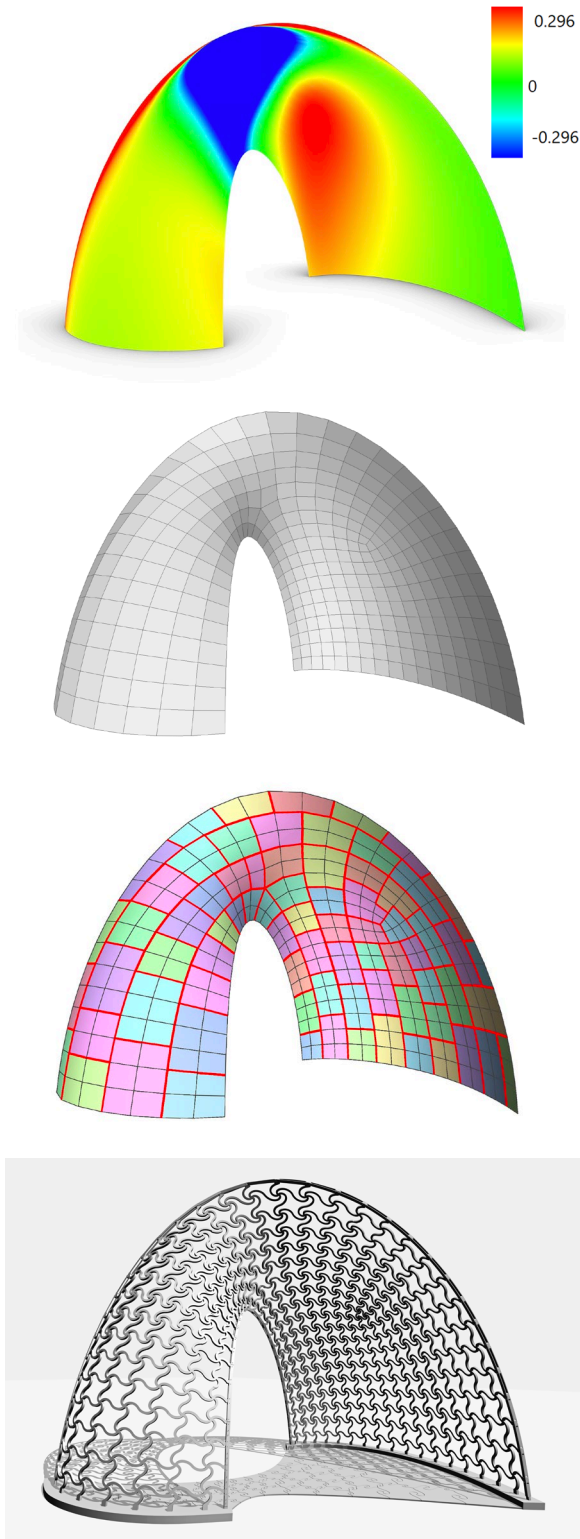


Figure 6: Computational design, from top to bottom: Gaussian curvature, quad mesh, patches, final design.

of horizontal load is considered in the condition of environments without public access providing a value of $q_k = 0.30 \text{ kN/m}$ at the handrail height.

The stability is checked with a vertical uniformly distributed equivalent load of $q_{el} = 0.1 \text{ kN/m}^2$ on the outer surface of the shell. This load has not been combined with other load cases, except self-weight and pre-stress.

Since the structure is installed in an indoor environment, no other action is considered, i.e. wind forces, snow load, thermal actions. Seismic forces are not considered because of the flexibility and the lightweight nature of the structure. Finally, the structure is not designed to support general vertical live loading or construction loads.

The design values of the actions at the ultimate limit state (ULS) are deducted from the combinations EN 1990 and adopting national load combination factors (NTC18). For the serviceability limit state (SLS) the characteristic combination is considered (dead load and pre-stress included with unitary combination factors).

3. COMPUTATIONAL DESIGN

The computational design of FlexMaps structures relies on a displacement-based automated methodology [22-23], which can be summarized into three main steps: quad meshing, spirals' computation, and patching (Fig. 6).

In the meshing phase, the continuous shape is discretized into quad tiles that are as regular as possible and have approximately the same size. This process takes as input the quad size, which defines the size of the spiral as well because each quad embeds a unique spiral, whose endpoints are on the edge's mid sides. The adopted target quad edge size is 0.25 m, which is a compromise between fabrication feasibility and handling.

Having thus fixed the first geometric parameter of the spiral, the actual computation optimizes for the other two, twist and width, such that each spiral will have a specific stiffness to allow the overall actual shape reaching the target once assembled. This problem is solved using a complex bounded optimization, where the displacements of the spirals are computed through an approximated beam model. For aesthetic reasons, the space of variables has been additionally restrained to a constant width of 20 mm and a twist range of 100-250°. The upper twist limit has a further aim to avoid too dense spirals, which may result too close with respect to the milling tolerance. The lower to avoid cross-like spirals.

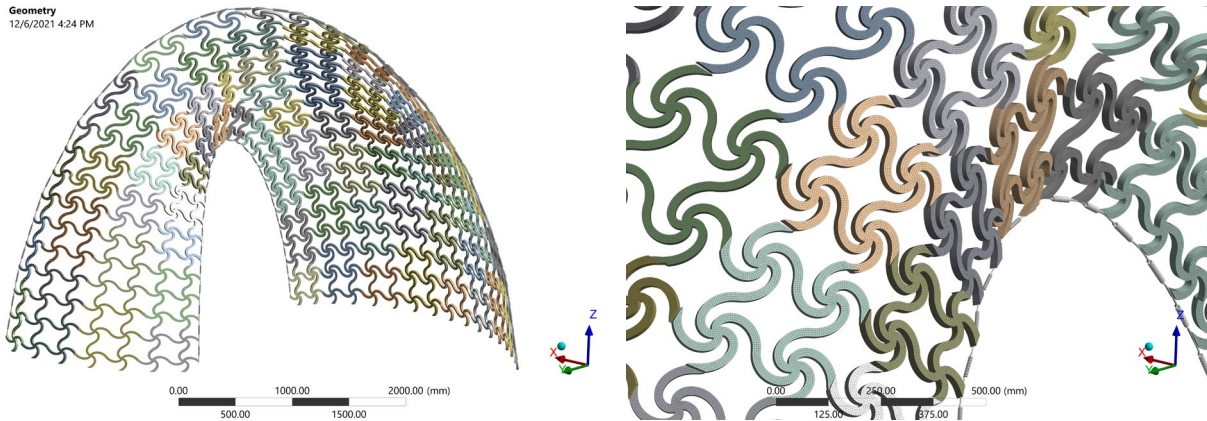


Figure 7: FE model of the structure at the starting point before pre-stress (i.e. where the panels are not in contact but are floating in the flat configuration. The springs, the boundary conditions and the internal restraints are birth/death elements).

The patching step manages the positioning of the seams on the shape, or similarly the quads that can be grouped to form a patch, and is related to: a) developability, i.e. the capacity of a surface to be unrolled with low/no distortion; and b) segmentation, i.e. creating patches whose size makes them fabricable and easy to handle. On this later point, the IAASS competition required all the components to fit into a maximum of six boxes up to 1.00x0.75x0.65 m and 32 kg each. Each patch is made of 2 up to 7 spirals for a total amount of 75 patches.

4. STRUCTURAL ANALYSIS

The simplifications introduced in the computational design and the lack of information concerning stress have raised the need for a detailed structural analysis. The structure has been previously analyzed for the exposition at the IAASS [25], and later the model has been detailed considering the more restrictive long-term installation at the Venice Biennale.

4.1. Finite element model

For the present case, a geometrically nonlinear solid model has been built and analyzed with the ANSYS package [26]. The model is generated with an automated workflow developed in conjunction with the algorithm employed for the computational design. The material model used in the analyses is linear elastic orthotropic, whose values are provided as per Sec. 2.3. The analysis is staged and consists of three consecutive load phases:

- *Pre-stress.* This load phase simulates the assembly of the patches made of 2 up to 7 spirals as they are individually bent and deformed to the target position. In this

phase, each panel is arranged in the closest-possible position to its target deformed shape. This initial placement avoids large rigid displacements and improves the convergence of the analysis reducing the load steps. Then, a displacement is imposed at the extremities of the spirals' free arms to bring them in their deformed position. Consequently, the patch assumes its pre-stressed configuration.

- *SLS loading.* This phase follows the previous one and aims to simulate the actual overall behavior of the structure in operating conditions. In this phase, the patches extremes are coupled, and boundary conditions are applied. In this setup, the structure behaves as a whole. Bonding conditions are applied to couple the patches, and other boundary conditions are applied, i.e. fixed support to the ground and springs to model the edge beams. Gravity is applied.
- *ULS loading.* In this phase, several and different ULS combinations of loads are appended to the previous phase.

The structure is modeled as a 3D system made of 3D elements SOLID185 (Fig. 7). The material properties are applied to each patch according to the direction of the fibers. The meshing used in the FE analyses is generated from a NURBS solid model. The patch-to-patch joint is simplified as a face-to-face contact, whose elements are modeled through CONTA174 and are activated using birth/death capacity from phase 2 forward. This simplification appears to be reasonable in evaluating global performances of the structure and because the

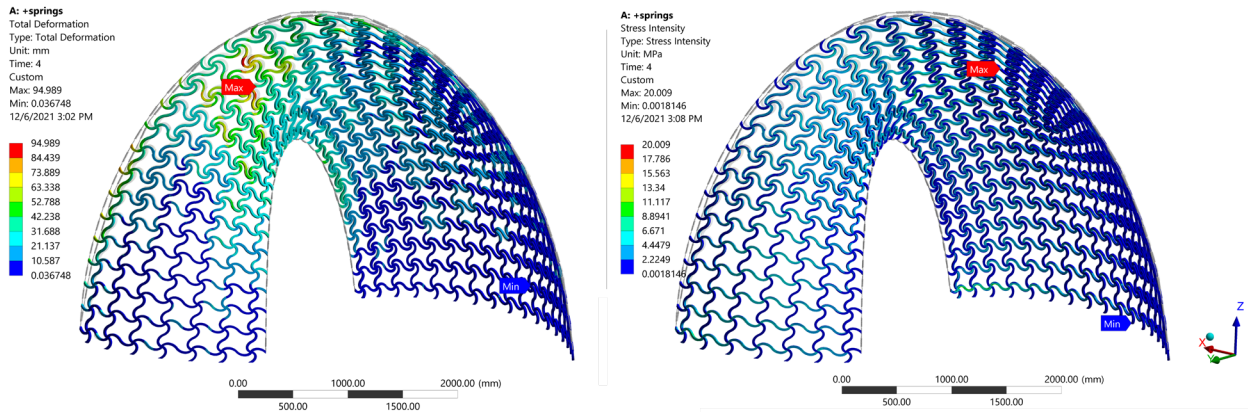


Figure 8: SLS results: on the left, displacement; on the right, stress intensity.

connection is designed to be stiff and resistant as the solid cross section.

The faces of the patches pointing down are restrained from phase 2 forward with fixed boundary conditions. The edge beams are modeled as springs having only axial stiffness with a remote attaching on the boundary faces. These elements are activated from phase 2 forward as well. Although these lamellae are bending-active components, their stiffness due to pre-stress is neglected on the safe side.

The stability analysis is performed through an eigenvalue buckling analysis from the results of a nonlinear analysis at ULS with q_{el} .

4.2. Analysis results

At the SLS, the structure exhibits a low deformation as shown in Fig. 8 in a range of 0–40 mm. This range of values has been deduced from the displacement of spirals' centers. The spirals' arms accumulate more deformation in pre-stressing, so they are excluded from this computation. For this kind of structure there is no limitation on the SLS displacement, however it is important to maintain the shape as close as possible to the target position to avoid second order effects. The stress intensity at the SLS shows that the material is well utilized (Fig. 8). The punctual strength verification is included in the next paragraph.

The accurate modeling through brick elements allows to accurately check not only the deformations but also the strength by means of punctual verifications. The spiral is submitted to a complex stress state that includes bending, tension or compression, shear, and torsion. Two of the most stressed patches are reported in Fig. 9. The strength verification is performed in the direction of the grain,

perpendicular to the grain, and in shear according to the NTC18. The analysis shows also peak values that are not considered because they are located at sharp features as produced by localized modeling inaccuracies and simplifications, i.e. spiral arms merging at the center, patch-to-patch joint, which are drawbacks of the automatic generation of the FE model. Overall, the safety of the patches is estimated to be sufficient for the intended use.

The stability of the structure results in a buckling multiplier of 1.83 (Fig. 10), which identifies a sufficient safety margin for such a temporary and indoor installation. This result appears remarkable considering that the structure is a lattice non-funicular shell, and so it has not high shape resistance.

4.3. Connections

A local model is developed to assess the strength of the connection with respect to the ultimate capacity of the section forces provided by the incident spiral arms. The model is depicted in Fig. 11 The fiber direction is aligned with the X axis. The material adopted for bolts is common structural steel. The extremity face on the left is restrained for all displacement, while the following ultimate loads have been applied to the right face:

$$F_x = \pm 3.32 \text{ kN}$$

$$F_y = 1.14 \text{ kN}$$

$$F_z = 1.14 \text{ kN}$$

$$M_y = \pm 22.27 \text{ kNmm}$$

$$M_z = \pm 22.27 \text{ kNmm}$$

The results show that the connector is always over-resistant with respect to the spiral, and high stress that are beyond the material capacity are uniquely

located in the transition zone from the 20 x 20 mm cross section of the spiral to the 25 x 25 mm of the connector or are localized peaks (Fig. 11).

The bolts worst case scenario occurs for F_z load, however the stress is well within the material capacity. Overall, the connector is safe and its

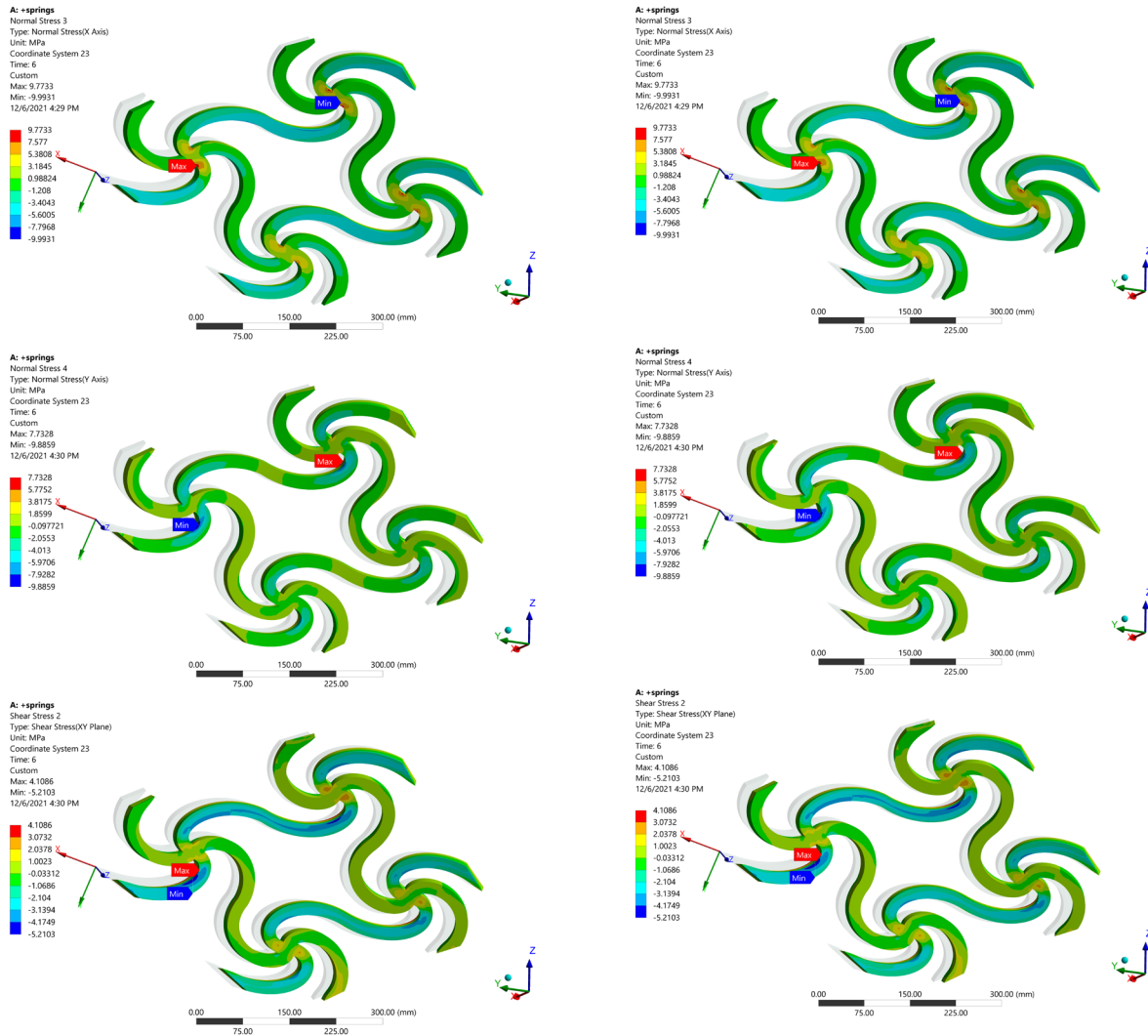


Figure 9: Patch 23 (left) and patch 15 (right) at ULS (with horizontal load): normal stress in X (top) and Y direction (middle), XY shear stress (bottom).

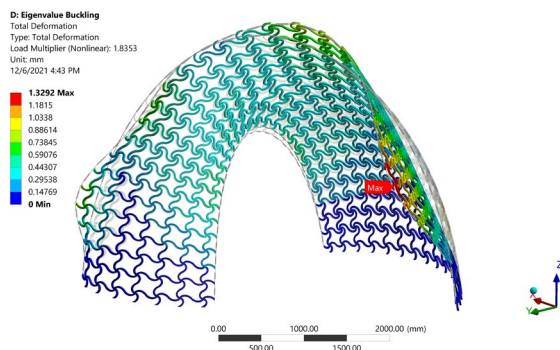


Figure 10: Buckling shape for the load factor of 1.8353, eigenfrequency analysis.

performances can be considered satisfactory. The sliding and the lifting are safely avoided by screwing the ground profiles to the supporting platform. The overturning is inherently avoided due to the spatially arrangement of the system, however the anchoring provides redundancy to the connection. The system was already self-equilibrated in the IAASS setup where only the paving provided sufficient balance to the supports forces.

The T-shaped footing loads are in the order of 100 times smaller than the full section capacity (Fig. 11). Therefore, the supports are able to safely support the design loads. The supports conditions are compression only faces on all sides of the largest part of the T.

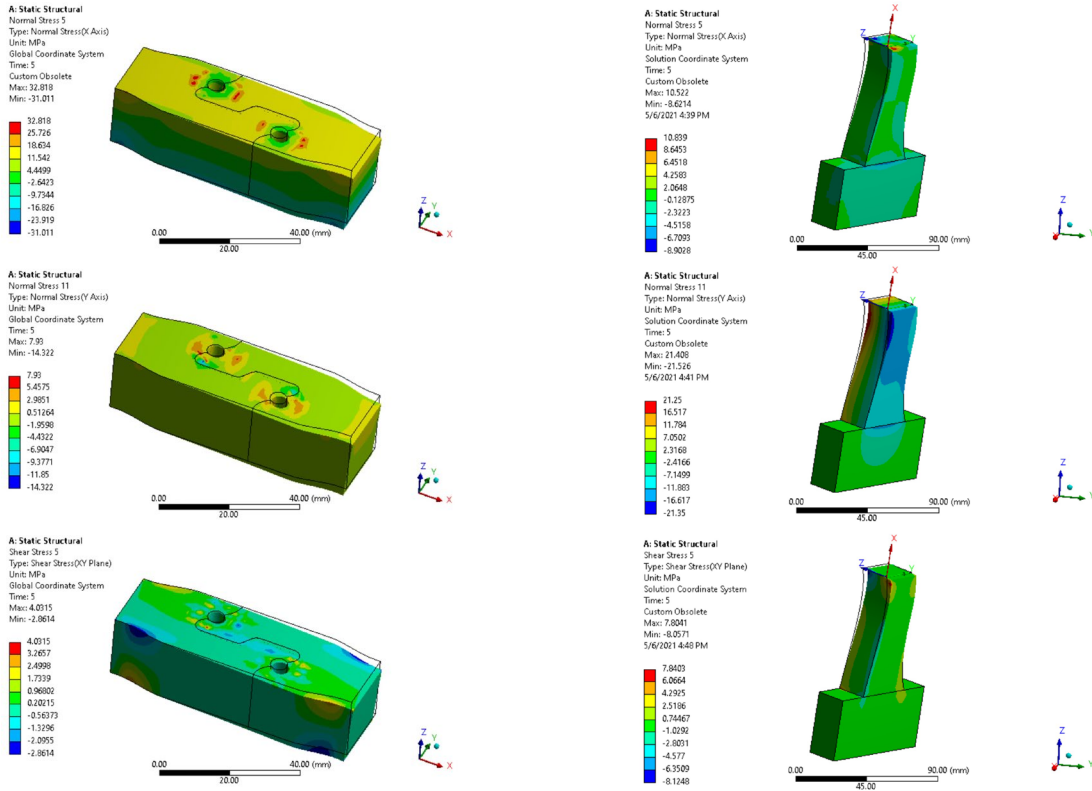


Figure 11: Patch-to-patch connection (left, bolts hidden) and T-footing (right), loaded by M_y : normal stress in X (top) and Y direction (middle), XY shear stress (bottom).

5. CONSTRUCTION

5.1. Fabrication

The FlexMaps patches and components have been fabricated with a 3-axes milling machine starting from raw plywood panels of 1.5 x 3.0 m, 20 mm thick. In this subtractive fabrication process, the main information to provide to the machines is the elements' outline to distinctively identify tool paths (Fig. 12).

A CAM file is produced by assigning a specific tool and cutting speed for each path. In the present case, two settings have been selected for the interfaces of the patch-to-patch joint (3 mm diameter tool with 1.5 mm depth penetration) and the rest (6 mm diameter tool). The connectors have been previously tested to find a proper tolerance, which resulted in 0.13 mm on each side of the contour. The third tool setting has been used to carve a numeric label on each spiral to facilitate the assembly.

5.2. Assembly (and disassembly)

The Pavilion is assembled element by element going from the larger ground beam to the other. Each patch is sequentially bent and fastened to the neighboring ones. Accordingly, the structure gradually moves to

the target global shape while gaining stiffness, as shown in Fig. 13. The edge beams play a fundamental role in this phase restraining the boundaries. Lastly, the structure is rigidly fixed on the supporting platform.

Conversely, to disassemble the structure it is necessary to release the restraint provided by the smaller edge beam in order to reduce the stiffness and disconnect all the elements one by one going backwards to the larger one.

All these steps are performed manually and are associated with several chances of failures (Fig. 14). Firstly, a major issue is represented by the exact sequence of assembly, which has not been pre-determined and has been referred to empirical evaluations. From the output of the FE simulation, the panels result resistant enough to be mounted but their assembly sequence is purely ideal. For that reason, to avoid failure, each element should be kept as close as possible to its final (assembled) position as any forced displacement may turn into breakage. To guarantee this condition and to avoid using a large temporary scaffolding and working at height, we tested as an effective procedure not to fix the first ground beam and allow rotation until almost all the



Figure 12: Fabrication of the FlexMaps patches.

patches are placed. Failure by traction or by bending (positive normal stress) as in Fig. 14a occurred when the patches were not connected sequentially, or they have been moved too far from their target position.

The patches are extremely easy to be jointed if they are not under stress, while the difficulty increases if they are bent. In both the assembly and disassembly, the friction between the interfaces of the connectors and the deformed configuration can lead to delamination as in Fig. 14b.

Except for limited cases (Fig. 14c), these failures are not reversible or negligible, and the component has to be replaced since a localized damage or restored parts constitute a stiffness alteration of the structure and could lead to a different equilibrium configuration. A limitation of such system, which is made of custom elements, is that failure can occur anywhere and there is no chance to rely on universal supply parts. Moreover, failures can be also triggered by material flaws.

6. VALIDATION AND MONITORING

The construction of the FlexMaps Pavilion as a large-scale demonstrator offered the opportunity to validate the design methodology. The real shape obtained through photogrammetry survey can be used for comparison with the FE results. Additionally, repeating the surveys in time can provide information on the evolution of the shape during the exhibition duration. Photogrammetry is a highly convenient technique as it requires only to take a set of photos of the object from different positions.

While photogrammetry could be able to densely reconstruct the whole geometry of the structure, due to the thinness of the spirals and the flat appearance of the surfaces, the resulting point cloud would probably be too noisy and scattered to be effectively compared with the CAD FE model. For this reason, we decided to track a specific set of points using markers.

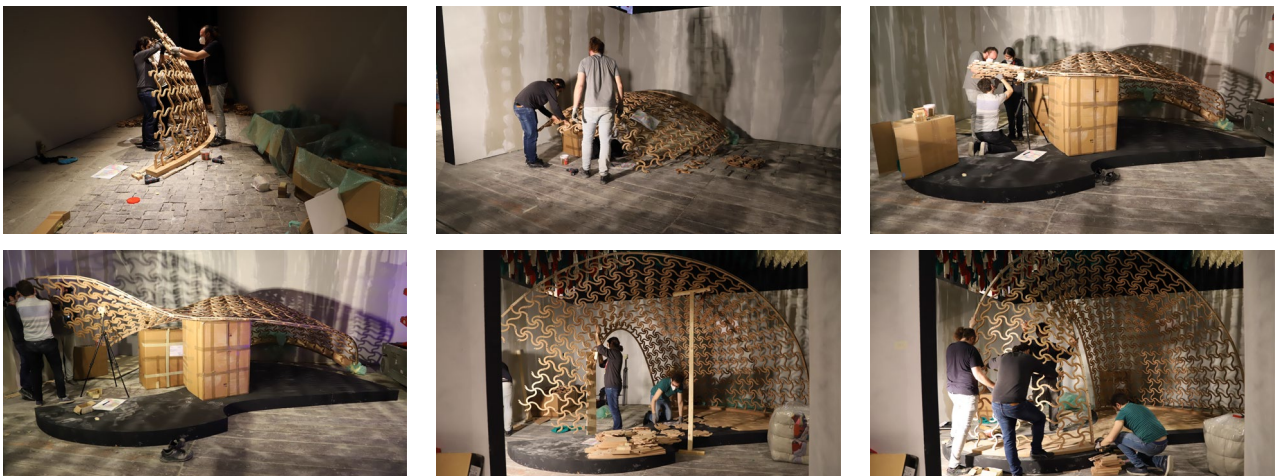


Figure 13: Assembly of the FlexMaps Pavilion at the Biennale

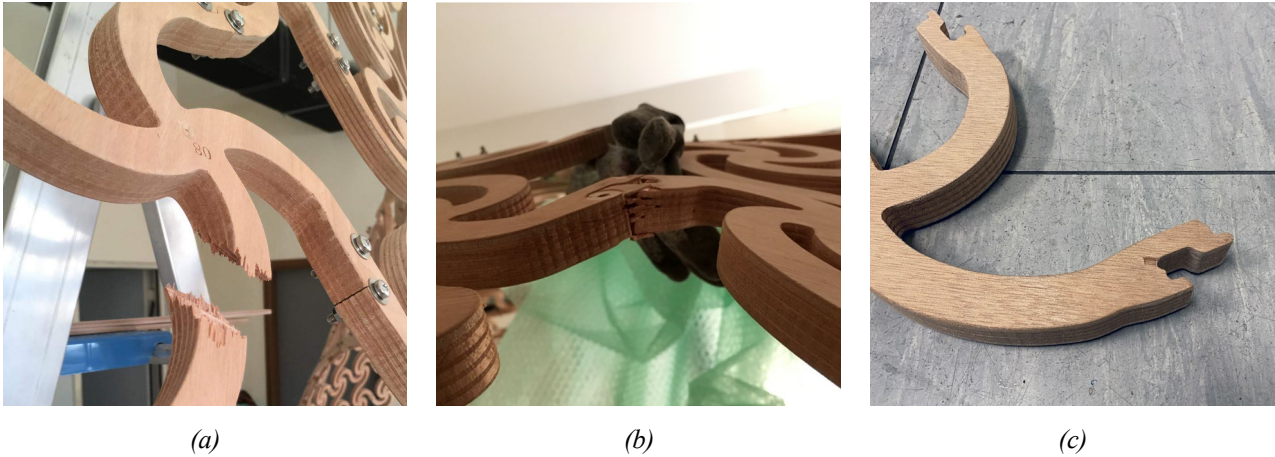


Figure 14: Failure cases occurring during assembly/disassembly: (a) traction/bending; (b) delamination; (c) minor failures.

In total, 48 markers (printed coded targets) have been affixed to both the base and the center of specific spirals all over the structure (Fig. 15). Since the base panels are fixed to the ground and will not move from one survey to the next, the 6 markers on the base act as Ground Control Points, to establish position, orientation, and scale of the photogrammetric surveys. The markers on the spirals are the points that will be measured and tracked across surveys.

The photogrammetric reconstruction is carried out in Agisoft Metashape [27]. The markers are automatically recognized by the software, and act as both "helpers" in the calibration/orientation of the photos (their location is used as a high-precision correspondence between input photos) and as "probes" (their position is determined in the reconstruction process).

In total, the survey has been repeated three times, using the same setup of markers and a consistent set of photos (in terms of number of photos, general positioning, camera used and its parameters). The precision of the reconstructions does satisfy the requirements of the monitoring process: matching residuals for the markers are below 1.8 pixels, and residuals for positional and scaling are below 1 mm.

At zero time (May 2021, after the assembly), the as-built structure presents a large misalignment from the FE deformed shape (Fig. 16), which is related to three main factors. Firstly, the ground beams relative distance has not been set accurately and it is larger than expected. Therefore, this error propagates, and the pre-stress of the patches is accordingly affected. Secondly, the accuracy of the shape depends uniquely on manual operations, on tolerances of the elements and on the guiding provided by the edge and ground beams. Therefore, a small error can

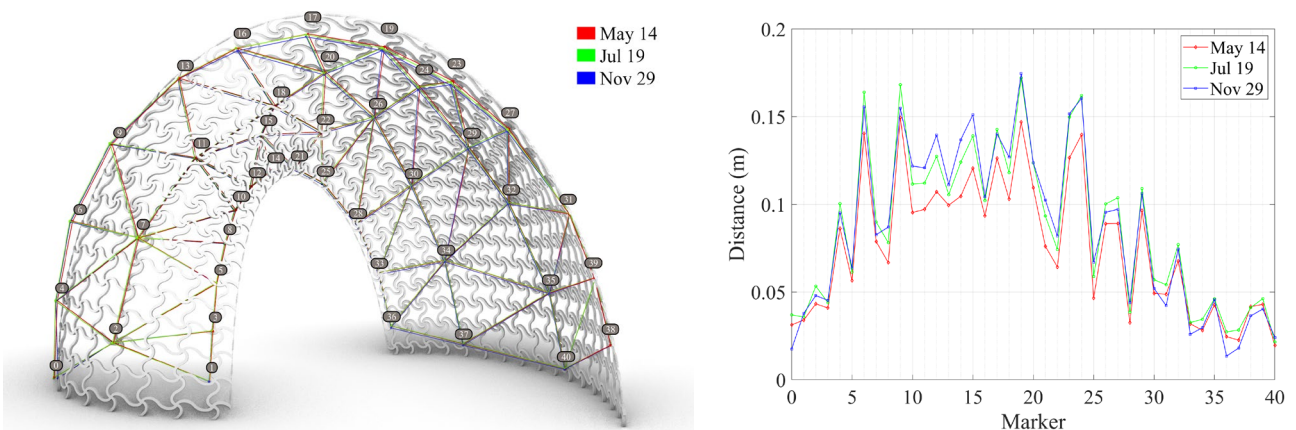


Figure 16: Photogrammetry validation and monitoring: on the left, comparison of the expected FE deformed shape (solid model) with the actual surveyed shapes (colored, the graph connecting the points has only a visualization purpose); on the right, histogram of the distances (surveyed-expected).

unfavorably turn into large shape deviations. Thirdly, the edge beams' bending stiffness and pre-stress are not negligible in practice, and because of their constant cross section they push the inner and outer arch-shaped boundaries towards a rounded profile. Therefore, the as-built shape appears less pointed than expected.

This survey has been repeated to measure the effect of long-term exposure to humidity under constant load as it can accelerate the decrease of mechanical properties and long-term strength. Indeed, a shape softening is observed, and the displacement increases on average by 0.022 m in July 2021, and by 0.041 m in November 2021 (with respect to July).

From a visual check, the patches are not affected by breakages caused by long-terms effects. But, after disassembling the structure, they present a residual inelastic deformation as shown in Fig. 17 that prevents them from recovering the flat configuration. This result suggests that stiffness and strength are reduced and the chances of failure by material flaws are increased. Unfortunately, the limitations of the FE model make the quantification of the actual stiffness loss by reverse-fitting unfeasible.



Figure 17: Inelastic deformation of patches after the Biennale exhibition.

7. CONCLUSIONS AND LIMITATIONS

The FlexMaps Pavilion has represented the first attempt to adopt bending-active metamaterial structures at the architectural scale and to monitor its behavior over a significant lapse of time. The shape of this structure has been selected with large design freedom, nonetheless its actualization reached a satisfying safety level as evidenced by the FE results and the verified behavior during the prolonged exposition at the Venice Biennale.

There are still open issues that should be considered

to overcome the present limitations. In particular, the FE model strategy could be improved by considering properly the edge beams. In the assembly phase, a more effective base positioning or the introduction of some basic shape checks can positively affect the overall shape and behavior of the structure.

Regarding the structural behavior, improvements can be introduced to make this kind of structures definitively applicable for more general load-bearing purposes. By design, the spiral patches have a limited and highly variable membrane stiffness, which is convenient to reach the assembled configuration but could be not enough safe for a more considerable SLS load or other loading scenarios. Moreover, the shape design could not be completely unrestricted and shall consider the future behavior of the structure, i.e. being funicular shape. For instance, this is not applicable in the present case since the shape is not funicular, so as a lattice structure it will not have large stiffness for a larger SLS load, and any (undesired) further bending will be allowed.

On the material side, plywood has remarkable advantages from the fabrication point of view, but it introduces several problems as a layered anisotropic creep-sensitive material. From a stiffness perspective, the patch strength is affected by its positioning during the milling with respect to the base-material sheet orientation. From the material flaws perspective, the layers represent a weak spot for propagating failures and the narrow width of the spirals have the potential of increasing this effect ('short grain effect'). Ultimately, as evidenced from the monitoring results, plywood softens when exposed to constant long-term loads and humid conditions, so evaluating different materials is recommended in the design phase of future FlexMaps structures.

ACKNOWLEDGMENTS

The FlexMaps Pavilion has been awarded First Prize at the "Competition and Exhibition of innovative lightweight structures" organized by the IAASS Working Group 21 within the FORM and FORCE, joint international conference of IAASS Symposium 2019 and Structural Membranes 2019 (Barcelona, 7-11 October 2019) with the following motivation: "for its structural innovation of bending-twisting system, connection constructability and exquisite craftsmanship"[28].

The FlexMaps Pavilion has been exhibited at the 17th International Architecture Exhibition (22 May-

21 November 2021), La Biennale di Venezia “How will we live together?” curated by Hashim Sarkis, Padiglione Italia “Resilient Communities” curated by Alessandro Melis, Vittorio Giorgini’s exhibition curated by Marco Del Francia [29].

The authors would like to acknowledge Bernd Bickel, Jesús Pérez, Emmanuel Iarussi, Eder Miguel; the Visual Computing Lab Staff of ISTI - CNR, in particular Massimiliano Corsini, Paolo Pingi; Antonio Rizzo of IPCF - CNR; the Administrative Staff of ISTI – CNR; and Antonio Chierici from our CNC service Manifattura Circolare.

This research was partially funded by the EU H2020 Programme EVOCATION: Advanced Visual and Geometric Computing for 3D Capture, Display, and Fabrication (grant no. 813170).

REFERENCES

- [1] N. Pietroni, D. Tonelli, E. Puppo, M. Froli, R. Scopigno, and P. Cignoni, "Statics aware grid shells," *Computer Graphics Forum*, 34(2), pp. 627–41, 2015. DOI: 10.1111/cgf.12590.
- [2] C. Jiang, C. Tang, H-P Seidel and P. Wonka, "Design and volume optimization of space structures," *ACM Trans Graphics*, 36(4):159:1–159:14, 2017. DOI : 10.1145/3072959.3073619.
- [3] N. Pietroni, M. Tarini, A. Vaxman, D. Panozzo and P. Cignoni, "Position-based tensegrity design," *ACM Trans Graphics*, 36(6):172:1–172:14, 2017. DOI: 10.1145/3130800.3130809.
- [4] M. Kilian, D. Pellis, J. Wallner, and H. Pottmann, "Material-minimizing forms and structures," *ACM Trans Graphics*, 36(6). DOI: 10.1145/3130800.3130827.
- [5] F. Gil-Ureta, N. Pietroni, and D. Zorin, "Reinforcement of general shell structures," *ACM Trans Graphics*, 39(5). DOI: 10.1145/3375677.
- [6] F. Laccone, L. Malomo, M. Froli, P. Cignoni, and N. Pietroni, "Automatic Design of Cable-Tensioned Glass Shells," *Computer Graphics Forum*, Vol. 39, No. 1, pp. 260-273, 2020. DOI: 10.1111/cgf.13801
- [7] M. Popescu, L. Reiter, A. Liew, T. Van Mele, R.J. Flatt, and P. Block, "Building in concrete with an ultra-lightweight knitted stay-in-place formwork: prototype of a concrete shell bridge," *Structures*, Vol. 14, pp. 322-332, 2018. DOI: 10.1016/j.istruc.2018.03.001
- [8] J. Brütting, J. Desruelle, G. Senatore, and C. Fivet, "Design of truss structures through reuse," *Structures*, Vol. 18, pp. 128-137, 2019. DOI: 10.1016/j.istruc.2018.11.006
- [9] C. Robeller, and N. Von Haaren, "Recycleshell: Wood-only Shell Structures Made From Cross-Laminated Timber (CLT) Production Waste," *Journal of the International Association for Shell and Spatial Structures*, 61(2), 125-139, 2020.
- [10] B. Bickel, P. Cignoni, L. Malomo, N. Pietroni, "State of the art on stylized fabrication," *Computer Graphics Forum*, 37(6):325–342, 2018. DOI:10.1111/cgf.13327.
- [11] X. Yu, J. Zhou, H. Liang, Z. Jiang, and L. Wu, "Mechanical metamaterials associated with stiffness, rigidity and compressibility: A brief review," *Progress in Materials Science*, 94:114–173, 2018. DOI: 10.1016/j.pmatsci.2017.12.003.
- [12] J. Lienhard, H. Alpermann, C. Gengnagel, and J. Knippers, "Active bending, a review on structures where bending is used as a self-formation process," *Int J Space Struct*, 28 (3–4) pp.187–96, 2013. DOI: 10.1260/0266-3511.28.3-4.187.
- [13] C. Gengnagel, E.L. Hernández, and R. B"auber, "Natural-fibre-reinforced plastics in actively bent structures," *Proc Inst Civil Eng- Constr Mater*, 166(6):365–77, 2013. DOI: 10.1680/coma.12.00026.
- [14] P. Nicholas, and M. Tamke, "Computational strategies for the architectural design of bending active structures," *Int J Space Struct*, 28(3–4), pp. 215–28, 2013. DOI: 10.1260/0266-3511.28.3-4.215.
- [15] J. Lienhard, *Bending-active structures: form-finding strategies using elastic deformation in static and kinetic systems and the structural potentials therein*, 36, Institut für Tragkonstruktionen und Konstruktives Entwerfen (ITKE). Universität Stuttgart 2014. DOI: 10.18419/opus-107.
- [16] J. Lienhard, and J. Knippers, "Bending-active textile hybrids," *J Int Assoc Shell Spatial*

- Struct*, 56(1), pp. 37–48, 2015. ISSN 1028-365X.
- [17] D. Sonntag, S. Bechert, and J. Knippers, "Biomimetic timber shells made of bending-active segments," *Int J Space Struct*, 32 (3–4):149–59, 2017. DOI: 10.1177/0266351117746266.
- [18] M. Tamke, Y.S. Baranovskaya, F. Monteiro, J. Lienhard, R. La Magna, M.R. Thomsen. "Computational knit – design and fabrication systems for textile structures with customised and graded CNC knitted fabrics," *Architect Eng Design Manage*, 1–21, 2020. DOI: 10.1080/17452007.2020.1747174
- [19] N. Kotelnikova-Weiler, C. Douthe, E.L. Hernandez, O. Baverel, C. Gengnagel, and J.F. Caron, "Materials for actively-bent structures," *Int J Space Struct*, 28(3–4), pp. 229–40, 2013. DOI: 10.1260/0266-3511.28.3-4.229.
- [20] R. La Magna *Bending-active plates: strategies for the induction of curvature through the means of elastic bending of plate-based structures*, 43, Institut für Tragkonstruktionen und Konstruktives Entwerfen (ITKE). Universität Stuttgart 2017. DOI: 10.18419/opus-9389.
- [21] J. Panetta, M. Konaković-Luković, F. Isvoranu, E. Bouleau, M. Pauly, "X-shells: a new class of deployable beam structures," *ACM Trans Graphics* 38(4). DOI: 10.1145/3306346.3323040.
- [22] L. Malomo, J. Pérez, E. Iarussi, N. Pietroni, E. Miguel, P. Cignoni, and B. Bickel, "FlexMaps: computational design of flat flexible shells for shaping 3D objects," *ACM Trans Graphics*, 241, 2018. DOI: 10.1145/3272127.3275076
- [23] F. Laccone, L. Malomo, N. Pietroni, P. Cignoni, and T. Schork, "Integrated computational framework for the design and fabrication of bending-active structures made from flat sheet material," *Structures*, Vol. 34, pp. 979-994, 2021. DOI: 10.1016/j.istruc.2021.08.004
- [24] F. Laccone, L. Malomo, J. Pérez, N. Pietroni, F. Ponchio, B. Bickel, and P. Cignoni, "FlexMaps Pavilion: a twisted arc made of mesostructured flat flexible panels," in *Proceedings of IAASS Annual Symposia* (Vol. 2019, No. 5, pp. 1-7). International Association for Shell and Spatial Structures (IAASS). (2019, October)
- [25] F. Laccone, L. Malomo, J. Pérez, N. Pietroni, F. Ponchio, B. Bickel, and P. Cignoni "A bending-active twisted-arch plywood structure: computational design and fabrication of the FlexMaps Pavilion," *SN Applied Sciences*, 2(9), pp. 1-9, 2020. DOI: 10.1007/s42452-020-03305-w
- [26] ANSYS. Academic Research Mechanical Release 18.0.; 2018.
- [27] AgiSoft Metashape Professional (Software). (2021). Retrieved from <http://www.agisoft.com/downloads/installer/>
- [28] IAASS Working Group 21 (organizers), "Competition and Exhibition of innovative lightweight structures", at the FORM and FORCE, joint international conference of IAASS Symposium 2019 and Structural Membranes 2019 (Barcelona, 7-11 October 2019): <https://www.jjo33.com/iass-barcelona-2019>
- [29] A. Melis, B. Medas, T. Pievani, *Catalogo del Padiglione Italia «Comunità Resilienti» alla Biennale Architettura 2021. Catalogo della mostra* (Vol. 1/b), D Editore, ISBN 8894830683